# The Nitrate Transporter Family Protein LjNPF8.6 Controls the N-Fixing Nodule Activity[1]

**Vladimir Totev Valkov,[a] Alessandra Rogato,[a] Ludovico Martins Alves,[a,2] Stefano Sol,[a,3] Mélanie Noguero,[b] Sophie Léran,[b,4] Benoit Lacombe,[b] and Maurizio Chiurazzi[a,5]**

[a]Institute of Biosciences and Bioresources, Institute of Biosciences and Bioresources (IBBR), Consiglio Nazionale delle Ricerche, 80131 Napoli, Italy

[b]Biochimie et Physiologie Moléculaire des Plantes, Centre National de la Recherche Scientifique Unité Mixte de Recherche/Institut National de la Recherche Agronomique/SupAgro/Université de Montpellier, Montpellier cedex 1, France

**ORCID IDs: 0000-0002-3811-0913 (V.T.V.); 0000-0002-0373-9076 (A.R.); 0000-0001-9924-3093 (B.L.); 0000-0003-2023-9572 (M.C.).**

N-fixing nodules are new organs formed on legume roots as a result of the beneficial interaction with soil bacteria, rhizobia. The nodule functioning is still a poorly characterized step of the symbiotic interaction, as only a few of the genes induced in N-fixing nodules have been functionally characterized. We present here the characterization of a member of the *Lotus japonicus* nitrate transporter1/peptide transporter family, *LjNPF8.6*. The phenotypic characterization carried out in independent *L. japonicus* LORE1 insertion lines indicates a positive role of LjNPF8.6 on nodule functioning, as knockout mutants display N-fixation deficiency (25%) and increased nodular superoxide content. The partially compromised nodule functioning induces two striking phenotypes: anthocyanin accumulation already displayed 4 weeks after inoculation and shoot biomass deficiency, which is detected by long-term phenotyping. LjNPF8.6 achieves nitrate uptake in *Xenopus laevis* oocytes at both 0.5 and 30 mM external concentrations, and a possible role as a nitrate transporter in the control of N-fixing nodule activity is discussed

Nitrate ($NO_3^-$) and ammonium ($NH_4^+$) represent the main forms of inorganic nitrogen source for plant growth and metabolism, with $NO_3^-$ being the largely dominant supply form in temperate climates (Miller and Cramer, 2005). Higher plants possess two $NO_3^-$ transport systems to cope with a wide range of external concentrations, the low-affinity transport system (greater than 0.5 mM) and the high-affinity transport system (less than 0.5 mM), both including constitutive and inducible types of transport (Tsay et al., 2007). In higher plants, low-affinity transport system proteins are represented mainly by the Nitrate Transporter1/Peptide Transporter Family (NPF), which includes a large number of genes (53 members in Arabidopsis [*Arabidopsis thaliana*] and 80 in rice [*Oryza sativa*]), divided in eight subfamilies and able to transport different substrates (Léran et al., 2014). To date, nitrate transport activity has been reported for 17 out of 53 NPF proteins in Arabidopsis (Corratgé-Faillie and Lacombe, 2017), with AtNPF6.3 being the only exception, as it displays dual affinity for nitrate in the high and low concentration ranges (Liu et al., 1999). Dual affinity for $NO_3^-$ uptake in *Xenopus laevis* oocytes also has been reported for the *Medicago truncatula* MtNPF6.8 (Morère-Le Paven et al., 2011) and MtNPF1.7 (previously named Numerous Infection and Polyphenolics/Lateral root-organ Defective; NIP-LATD) proteins (Bagchi et al., 2012). Moreover, Mtnpf1.7 knockout (KO) mutant plants display more defective lateral root responses in planta at low $KNO_3$ concentrations than at higher concentrations, indicating a high-affinity transport physiological function (Bagchi et al., 2012). The specificity of the spatiotemporal patterns of AtNPF expression and their regulatory profiles ensure nitrate

[1] This work was supported by grants from the Italian Ministry of Education (Progetti di Rilevanza Nazionale, PRIN 2010/2011, PRO-ROOT, Prot. 20105XLAXM), from Rete delle Biotecnologie in Campania, Progetto Bio Industrial Processes – BIP – CUP B25C13000290007, from the Institut National de la Recherche Agronomique (Contrat Jeune Scientifique Ph.D. Fellowship to S.L.), and from the Agence Nationale de la Recherche (ANR-14-CE34-0007-01-HONIT with a postdoctoral fellowship to M.N.). L.M.A. was supported by a Short-Term Fellowship from the European Molecular Biology Organization.

[2] Current address: Buchmann Institute for Molecular Life Sciences, Goethe University Frankfurt, Max-von-Laue-Strasse 15, 60438 Frankfurt, Germany.

[3] Current address: CEINGE Biotecnologie Avanzate, Napoli, Italy; and Department of Biology, University of Naples Federico II, 80145 Napoli, Italy.

[4] Current address: Interactions Plantes Microorganismes Environnement, Unité Mixte de Recherche Centre de Coopération Internationale en Recherche Agronomique pour le Développement/Institut de Recherche pour le Développement/Université Montpellier, 911 avenue Agropolis, BP64501, 34394 Montpellier cedex 05, France.

[5] Address correspondence to maurizio.chiurazzi@ibbr.cnr.it.

The author responsible for distribution of materials integral to the findings presented in this article in accordance with the policy described in the Instructions for Authors (www.plantphysiol.org) is: Maurizio Chiurazzi (maurizio.chiurazzi@ibbr.cnr.it).

All authors critically revised the article; V.T.V., A.R., L.M.A., M.N., S.S., and S.L. performed research and analyzed data; B.L. and M.C. designed research; M.C. conceived the project and wrote the article.

www.plantphysiol.org/cgi/doi/10.1104/pp.17.01187

  

uptake from soil, long-distance transport within the plant body, and distribution from source to sink tissues (Krapp et al., 2014; Noguero and Lacombe, 2016).

It is well known that nitrate also plays a role as a signaling molecule involved in the control of many physiological processes, including gene regulation (Wang et al., 2004) and root development (Walch-Liu et al., 2006). A crucial role in the nitrate signaling pathway governing root system architecture and modulation of the expression of many genes has been demonstrated for AtNPF6.3, which functions as a nitrate transceptor (Ho et al., 2009; Krouk et al., 2010). In particular, the control exerted by AtNPF6.3 on lateral root development, in response to different external nitrate concentrations, is mediated by its action as an auxin transport facilitator (Krouk et al., 2010; Bouguyon et al., 2015). Plant NPF members encompass proteins capable of transporting different substrates other than nitrate, such as di/tripeptides, amino acids, glucosinolates, malate, auxin, abscisic acid (ABA), $GA_3$, and jasmonic acid (Frommer et al., 1994; Jeong et al., 2004; Waterworth and Bray, 2006; Krouk et al., 2010; Kanno et al., 2012; Nour-Eldin et al., 2012; Saito et al., 2015; Tal et al., 2016). In particular, the multitransport feature recently reported for some NPF proteins displaying phytohormone transport capacities may suggest additional roles played by these proteins in regulatory cross talk linking different physiological signals (Krouk et al., 2010; Kanno et al., 2012; Chiba et al., 2015; Saito et al., 2015; Tal et al., 2016). However, the different transport capacities are distributed among the eight NPF subclades identified in plants (Léran et al., 2014), as sequence homologies do not correlate with substrate specificity and the determination of the transported substrate cannot be determined from the sequence data alone.

Symbiotic nitrogen fixation (SNF) is part of a multistep mutualistic relationship, mainly restricted to legumes, in which plants provide a niche (represented by root nodule organs) and fixed carbon to the microorganism partner (*Rhizobium* spp.) in exchange for fixed nitrogen. The establishment and functioning of an effective SNF consists of the reciprocal recognition of symbiotic partners, penetration, stimulation of cortical cell division (nodule primordium), invasion of divided cells, differentiation of the endosymbiont, N fixation, and nodule senescence. As for the root system, nitrate, both as nutrient and signal, plays a regulative role in the nodulation program, and high external concentrations inhibit different steps of SNF, although the mechanisms involved are still controversial (Carroll and Gresshoff, 1983; Carroll and Mathews, 1990; Fujikake et al., 2003; Barbulova et al., 2007; Omrane and Chiurazzi, 2009; Jeudy et al., 2010). The addition of 5 mM nitrate quickly stops nodule growth, and this effect seems to be linked to a decrease in photoassimilate supply to growing nodules (Fujikake et al., 2003). Furthermore, N-fixation activity is almost completely lost after a short exposure to high nitrate concentrations (Schuller et al., 1988; Vessey and Waterer, 1992), and several hypotheses have been offered to explain such a strong impact of nitrate on nodule activity (Vessey and Waterer, 1992; Minchin, 1997; Naudin et al., 2011; Cabeza et al., 2014).

In N-fixing nodules, bacteria that enter root nodule cells are surrounded by a plant-derived membrane, the peribacteroidal membrane (PBM), which encloses the intracellular bacteria in a symbiosome. Inside the symbiosome, bacteria differentiate into bacteroids with the ability to fix atmospheric $N_2$ via nitrogenase activity. A primary nutrient exchange across the PBM is the transport of carbon energy as products of plant photosynthates to bacteroid in exchange for fixed nitrogen. N fixation is an energy-intensive process that also requires oxygen for respiration to generate ATP and reducing equivalents for the reduction of $N_2$ to $NH_3$. At the same time, as bacteroid nitrogenase is inactivated by oxygen, a microaerophilic condition must be maintained in rhizobia-containing nodule cells. This is achieved by limiting the rate of oxygen influx through the outer uninfected cell layers of the nodule (Witty and Minchin, 1998) and by maintaining high rates of respiration in mitochondria and bacteroids of invaded cells (Bergensen, 1996). High respiration rates are ensured mainly by the presence at millimolar concentrations of the high-affinity oxygen-binding protein leghemoglobin, which delivers oxygen efficiently to mitochondria and bacteroids for respiration while buffering free oxygen at the required level (Appleby, 1984). This extremely high rate of respiration in the invaded nodule cells is the main reason for reactive oxygen species (ROS) generation, whose steady-state concentrations must be strictly controlled, as these represent not only toxic by-products of aerobic metabolism but also key signals for nodulation. Nodule-specific metabolic pathways are completed by redox reactions involved in the control of concentrations of ROS generated in $N_2$-fixing nodules (Evans et al., 1999; Hernandez-Jimenez et al., 2002; Puppo et al., 2005; Becana et al., 2010; Matamoros et al., 2013). The distinct metabolic pathways of $N_2$-fixing nodules reflect changes in gene expression for related metabolic enzymes. Genome-wide transcriptomic analyses have allowed the classification of genes induced in nitrogen-fixing nodules, and among these, a significant percentage of genes encoding for transporter proteins have been found (Colebatch et al., 2004; Hogslund et al., 2009; Takanashi et al., 2012). NPF proteins are largely represented in this category of transporters, and at least eight members have been recently subclassified as nodule-induced (NI) genes in *Lotus japonicus* (Valkov and Chiurazzi, 2014).

Here, we report the functional characterization of *LjNPF8.6*, an NI gene that plays a specific positive role on nodule functioning controlling nitrogenase activity and nodular ROS content.

## RESULTS

### LjNPF8.6 Expression Is Induced Progressively in N-Fixing Nodules

We previously reported the identification of a large *L. japonicus* NPF family consisting of more than 70 members, 39 of which have a complete sequence that can be

retrieved from the *L. japonicus* whole-genome sequence resource (Sato et al., 2008; Valkov and Chiurazzi 2014; http://www.kazusa.or.jp/lotus/). Transcriptomic data provided through gene-specific and GeneChip approaches (Hogslund et al., 2009; Criscuolo et al., 2012; Takanashi et al., 2012) allowed the identification of a subclass of eight NPF genes with a clear-cut NI level of expression (Valkov and Chiurazzi, 2014). Among these, the gene Lj3g3v2681670.1 (genomic assembly build 3.0, classified as chr2LjT15I01.230.r2.d in build 2.5) has been subclassified in clade 8 and provisionally named *LjNPF8.6* (Valkov and Chiurazzi, 2014), which encodes for a 561-amino acid protein with a molecular mass of 62.4 kD.

In order to further characterize the profile of expression of *LjNPF8.6*, we first analyzed the distribution of the *LjNPF8.6* transcript in different organs of *L. japonicus* by quantitative reverse transcription (qRT)-PCR. Seedlings were germinated on Gamborg B5 medium without N sources, inoculated with *Mesorhizobium loti*, and RNA extracted from different organs after 4 weeks. The *LjNPF8.6* gene is expressed strongly in mature nodules, with an amount of transcript about 10-fold higher than in roots, whereas it is barely detectable in stems, leaves, and flowers (Fig. 1A). *LjNPF8.6* expression also has been tested through a time-course experiment in roots of *L. japonicus* inoculated with *M. loti* at 1 week after sowing. The *LjNPF8.6* expression pattern is not induced in roots at early times after *M. loti* inoculation when compared with the well-known early symbiotic marker *NODULE INCEPTION* (*LjNIN*) gene (Schauser et al., 1999). Moreover, a progressive increase of the amount of *LjNPF8.6* transcript is detected in nodule tissue at 10 and 28 d after inoculation (Fig. 1B). This profile of induction, starting after the onset of N fixation and induced progressively during nodule maturation, resembles that of the late nodulin genes, suggesting an involvement in nodule functioning rather than development.

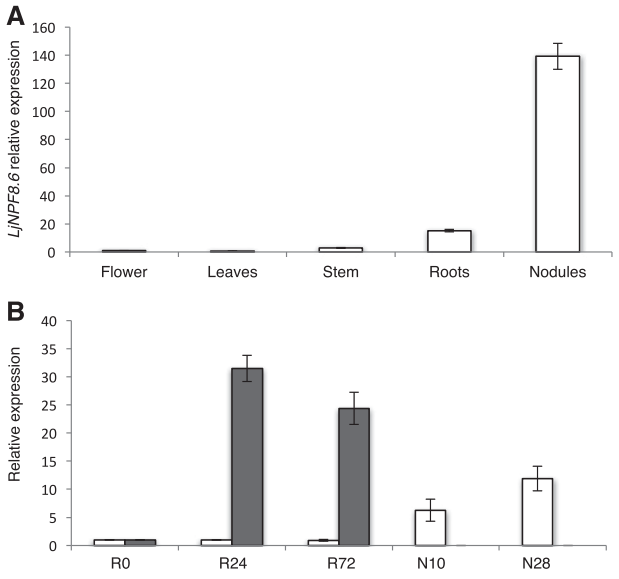


**Figure 1.** *LjNPF8.6* transcriptional regulation. A, Expression in different organs. RNAs were extracted from wild-type plants grown on Gamborg B5 derivative medium without N source at 4 weeks post inoculation (wpi). Mature flowers were obtained from *L. japonicus* plants propagated in the growth chamber. B, Time course of expression in root and nodule tissues after *M. loti* inoculation. RNAs were extracted from roots of wild-type seedlings grown in N starvation conditions at different times after inoculation (R0, 24 h, and 72 h) and from young (10 d post inoculation) and mature (28 d post inoculation) nodules. Expression levels are normalized with respect to the internal control ubiquitin (*UBI*) gene and plotted relative to the expression of flowers (A) and R0 (B). White bars, *LjNPF8.6*; gray bars, *LjNIN*. Data bars represent means and SD of data obtained with RNA extracted from three different sets of plants and three real-time PCR experiments.

### Isolation of LORE1 Insertion Null Mutants and Phenotypic Characterization

To determine the in vivo function of *LjNPF8.6*, three independent LORE1 insertion mutants have been isolated from the LORE1 line collection (Fukai et al., 2012; Urbański et al., 2012; Malolepszy et al., 2016). Lines 53155, 49638, and 19899, bearing retrotransposon insertions in the second and third exons (Fig. 2), have been genotyped by PCR, and plants homozygous for the insertion event into the *LjNPF8.6* gene were selected and transferred to the plant chamber for seed production. End-point reverse transcription-PCR revealed no detectable *LjNPF8.6* mRNA in mature nodules of homozygous plants screened from lines 53155, 49638, and 19899; hence, these can be considered null mutants (Supplemental Fig. S1). Initially, two individual homozygous mutant plants from each line were selected for analyses, and because their growth phenotypes did not differ significantly, the data obtained with the selected individual mutants were pooled in this study. The initial phenotyping of the three *LORE1* mutant lines included measurements of shoot lengths and fresh weights of 4-week-old plants with and without inoculation with *M. loti*. As shown in Figure 3, in the absence of N sources (no N) or in the presence of $KNO_3$ concentrations (100 $\mu$M, 1 mM) compatible with full nodulation capacity, the three lines did not present significant differences, when compared with wild-type plants, in terms of shoot biomass and nodule number (Fig. 3). In order to test whether LjNPF8.6, which also is expressed at a significant level in the root tissue, could be involved in the nitrate-dependent inhibitory pathways controlling the nodule formation process, nodulation capacity also was tested in the presence of high external concentrations of $KNO_3$ (10 mM). As expected, the number of nodules is reduced strongly in *L. japonicus* wild-type plants (85%; Barbulova et al., 2007), and an identical inhibitory response is observed in the *Ljnpf8.6* mutants (Fig. 3C).

However, a careful analysis of phenotypes of the inoculated plants allowed us to detect a visible accumulation of anthocyanin, conferring deep purple color, in stems of mutant plants in symbiotic conditions when compared with wild-type plants (Fig. 4, A and B). The

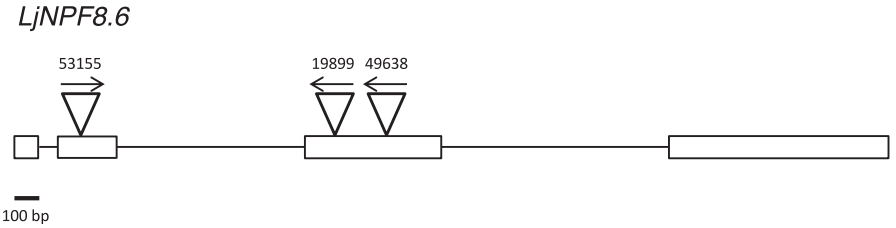


**Figure 2.** Exon/intron organization of the *LjNPF8.6* gene. Insertion sites and relative orientations of the LORE1 retrotransposon element in the 53155, 19899, and 49638 lines are indicated.

anthocyanin accumulation starts to be easily detectable in inoculated *Ljnpf8.6* plants at 17 to 20 d after inoculation, and the spreading of pigments increases progressively up to the third internode (40%–45% of the stem length) at 4 wpi, whereas in wild-type plants, traces of pigmentation are observed only at the base of the stem structure (Fig. 4, A and B). A quantitative analysis performed through anthocyanin extraction from stem tissues at 4 wpi revealed a content 210% to 250% higher in nodulated KO than in wild-type plants grown either under no N or 1 mM $KNO_3$ conditions (Fig. 4C). A significant systemic increase of anthocyanin content also is revealed in roots of mutant plants inoculated with *M. loti* (Supplemental Fig. S2A). Conversely, uninoculated mutant plants did not display anthocyanin accumulation in stems and roots, as no quantitative differences were detected in wild-type and mutant plants grown in the presence of 1 or 5 mM $KNO_3$ (Fig. 4C; Supplemental Fig. S2A). Line 53155 was analyzed only for plants inoculated on 1 mM $KNO_3$ conditions and not utilized further for phenotypic characterization, because of the segregation of the $nod^-$ phenotype due to the additional LORE1 insertion in the *CERBERUS* gene (Yano et al., 2009). However, the identical phenotype displayed by the 53155, 49638, and 19899 lines confirms that the LORE1 insertion in the *LjNPF8.6* gene is the causal mutation of the increased anthocyanin content observed exclusively in symbiotic conditions. In addition, heterozygous plants for the LORE1 insertion in the *LjNPF8.6* gene, isolated in the three lines, did not display high levels of anthocyanin in the stem (data not shown).

### *Ljnpf8.6* Nodule Mutants Display Nitrogenase Activity Deficiency under Permissive Low-Nitrate Conditions, Associated with a Long-Term Shoot Biomass Reduction Phenotype

The accumulation of anthocyanin is a clear marker of plant response to different stress conditions such as low N availability (Diaz et al., 2006). In order to investigate whether the anthocyanin accumulation detected in the *Ljnpf8.6* mutant in symbiotic conditions is correlated with reduced nodule functionality, we compared N-fixation activity in nodules of wild-type and mutant plants at 4 wpi. A significant 25% decrease of acetylene reduction activity (ARA) is detected in nodules of *Ljnpf8.6* mutants grown either in the absence of N or in the presence of 1 mM $KNO_3$ (Fig. 5A). However, the reduction of N-fixation capacity detected in the *Ljnpf8.6* KO genetic background is not correlated with any evident shoot phenotype other than anthocyanin accumulation during in vitro growth, which must be limited to a short period of analysis (4 wpi; Fig. 3). In order to check whether a more severe shoot biomass phenotype could be displayed by the *Ljnpf8.6* mutants, 4-week-old nodulated plants were transferred in growth conditions compatible with long-term phenotypic analyses. We first tried to transfer the 4-week-old nodulated plants to pots filled with inert material, but the phenotyping analyses were biased by a random, genotype-independent stress response due to bad adaptation to the new conditions of growth. Conversely, the transfer of nodulated plants to hydroponic conditions minimizes this unpredictable plant phenotype, and all the plants could be scored for reliable shoot phenotypes after another 4 weeks. Figure 5, B and C, shows the striking shoot biomass-deficient phenotype displayed by the *Ljnpf8.6* mutants 4 weeks after transfer to hydroponic conditions (8 wpi). The two main representative phenotypes observed in all the inoculated mutant plants are stunted shoots with pale green and/or abscised leaves (Fig. 5, B and C).

### *Ljnpf8.6* Mutant Nodules Display Superoxide Overproduction

In *M. truncatula*, the NIP/LATD protein has been associated, through the characterization of the weak allelic mutant *nip-3*, with defects in bacteria release or proliferation within NI cells, where fewer bacteria are observed (Teillet et al., 2008). Therefore, we tested whether the deficient N fixation activity observed in the *Ljnpf8.6* nodules (Fig. 5A) is associated with a reduced invasion capacity. Seedlings grown in N starvation conditions were inoculated with an *M. loti* strain carrying a constitutively expressed *hemA*::*lacZ* reporter gene fusion for the staining of young and mature nodules. As shown in Figure 6, A to D, no differences were observed in the density of the invading *M. loti* strain in wild-type and mutant nodules.

Reduction of N-fixation activity in mature nodules also has been associated with oxidative damage provoked by ROS overproduction, which can be due to natural aging or to exposure to different stress conditions (Becana et al., 2010). We monitored superoxide ($O_2^-$) production at different stages of nodulation using the ROS-reactive dye nitroblue tetrazolium(NBT). The nascent nodule primordia are strongly stained in both

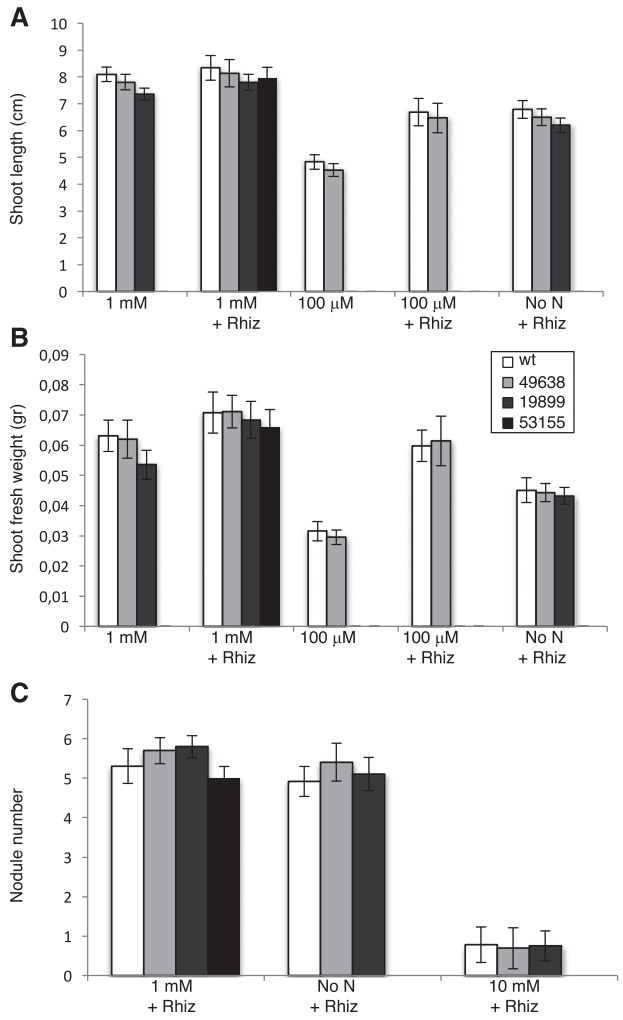


**Figure 3.** Quantitative analysis of shoot biomass and nodulation capacity of *L. japonicus* wild-type (wt) and *LjNPF8.6* null mutant plants, grown in the presence of different $KNO_3$ concentrations, in symbiotic and nonsymbiotic conditions. A, Shoot length per plant. B, Fresh shoot weight per plant. C, Nodule numbers per plant. The different $KNO_3$ concentrations and, when determined, *M. loti* inoculations are indicated. Bars corresponding to wild-type and different LORE1 plants are indicated. Data bars represent means and SE of measures from three experiments (12 plants per experiment per condition). Data in A and B were scored 25 d after sowing (21 d after transferring the plants from water agar). Data in C were scored 28 d after inoculation.

the wild type and mutants (Fig. 6, E and F), while, as nodules mature and enlarge in size, the staining intensity decreases strongly in both genotypes but remains more intense in mutant nodules (Fig. 6, G and H). In 60% of wild-type big nodules, the staining is not even detectable in whole-mount samples, whereas in all the comparable mutant nodules, this is still clearly visible. In whole-mount samples, NBT staining is confined to the lenticel structure on the nodule surface (Fig. 6, G and H). Longitudinal nodule sectioning has confirmed these differences of staining intensity in the parenchyma region (Fig. 6, I and J). The quantitative analysis conducted on mature nodules confirms a significant overall increase of $O_2^-$ content in the 49638 line compared with wild-type plants (25%; Fig. 6K). $O_2^-$ content also was quantified on root and stem tissues of inoculated plants, where no significant differences were observed (Supplemental Fig. S2B). These results indicate a local $O_2^-$ increase in the nodule organ.

### LjNPF8.6 Is a Nitrate Transporter

Nitrate transport activity has been reported for 17 out of 53 NPF proteins in Arabidopsis (Corratgé-Faillie and Lacombe, 2017), which have been characterized as low-affinity transporters, with the exception of AtNPF6.3/NRT1.1, which is a dual-affinity nitrate transporter (Ho et al., 2009; Krouk et al., 2010). In clade 8 of the plant NPF family (Léran et al., 2014), the only NPF member characterized up to now as a nitrate transporter when expressed in *X. laevis* oocytes is the rice OsNPF8.9 protein, which shares 45% amino acid identity with LjNPF8.6 (Lin et al., 2000). In order to assess whether *LjNPF8.6* encodes a nitrate transporter, in vitro-synthetized *LjNPF8.6* complementary RNA (cRNA) was injected into *X. laevis* oocytes for functional assay. Two days after the injections, oocytes were tested for nitrate $^{15}NO_3$ uptake activity at two different nitrate concentrations at pH 5.5: low (0.5 mM) and high (30 mM). *LjNPF8.6* cRNA-injected *X. laevis* oocytes were compared with the *AtNPF6.3*-injected oocytes. Both batches of oocytes display NPF-dependent $^{15}NO_3$ accumulation in 30 mM as well as 0.5 mM external nitrate (Fig. 7). Within this range of concentrations, a Michaelis-Menten fit leads to a $K_m$ of 7.8 mM, indicating an LjNPF8.6 low-affinity transport capacity (Supplemental Fig. S3), while a high-affinity capacity (low $NO_3^-$ concentrations) range was not tested.

The uptake activity observed in *X. laevis* oocytes (Fig. 7) prompted us to test for possible roles of LjNPF8.6 associated with the nitrate transport function important for nodule activity. Therefore, we checked whether LjNPF8.6 could play a role in the inhibitory pathway responsible for the abrupt decrease of nodule activity described after exposure to external high nitrate concentrations (Schuller et al., 1988; Vessey and Waterer, 1992). Wild-type and mutant nodulated plants (4 wpi) were transferred for 3 d in the presence of 10 mM $KNO_3$, and nodule activity was analyzed by ARA. The nitrogenase activity is inhibited at the same level in both wild-type and *Ljnpf8.6* plants, ruling out the hypothesis of LjNPF8.6 involvement in the signaling pathway inhibiting nodule functioning at high external nitrate concentrations (Fig. 5A).

Jeong et al. (2004) reported the identification of an NPF gene (AgDCAT1) expressed in nodules of *Alnus glutinosa* that encodes for a protein capable of malate transport in heterologous systems. Therefore, we also tested the capacity of LjNPF8.6 to transport malate, the carbon source supplied to bacteroids for metabolism and nitrogen fixation (Day and Copeland, 1991). LjNPF8.6 was cloned

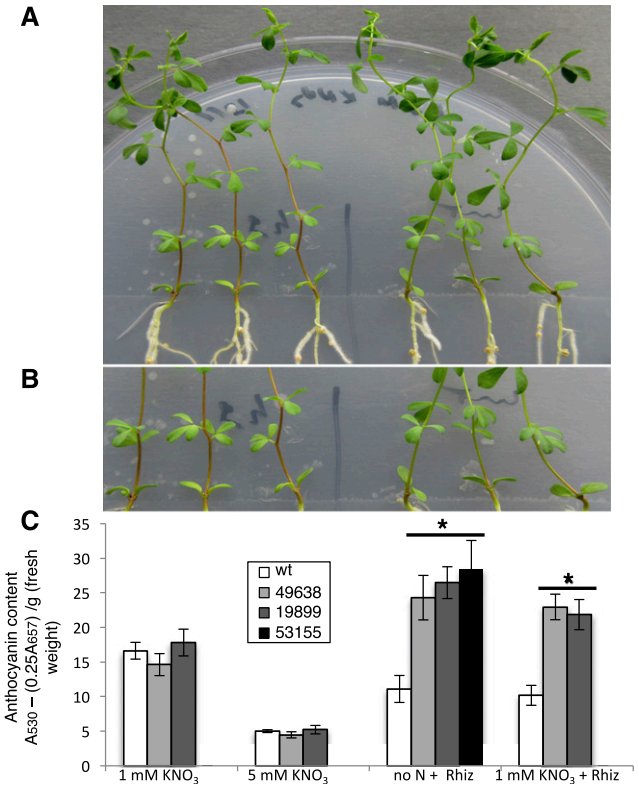


**Figure 4.** Analysis of anthocyanin content. A, Three representative wild-type and 49638 plants are shown on the right and left sides of the petri dish, respectively. B, Higher magnification showing intense purple colors in the stems of mutant plants (on the left). C, Anthocyanin content in stems of wild-type (wt) and LORE1 lines. The different $KNO_3$ concentrations and, when determined, *M. loti* inoculations are indicated. Bars corresponding to wild-type and different LORE1 plants are indicated. Data bars represent means and SE of measures from three experiments (12 plants per experiment per condition). Data in C were scored 28 d after inoculation. Asterisks indicate significant differences ($P < 0.001$) from wild-type levels.

into the *Escherichia coli* expression vector pKK223-3 under the control of the tac promoter (Brosius and Holy, 1984), and the resulting plasmid was used to transform the dicarboxylate transport mutant CBT315 strain (*dctA*; Lo et al., 1972). Functional complementation was tested on M9 medium with 10 mM malate as the sole carbon source with or without isopropylthio-β-D-thiogalactoside as an inducer of the tac promoter, and the Arabidopsis gene AtALMT6 (At2G17470), encoding a member of the aluminum-activated malate transporter family, was used as a positive control (Meyer et al., 2011). We did not observe any growth of the CBT315 strain transformed with the LjNPF8.6-expressing plasmid, while At2G17470 was able to complement the malate transport defect (Supplemental Fig. S4). This negative result suggests that LjNPF8.6 does not encode for a malate transporter, although we cannot exclude that the *L. japonicus* protein is not correctly expressed and/or addressed to the plasma membrane in *E. coli*.

### *Ljnpf8.6* Mutants Have Unaltered Nitrate Content in Different Plant Organs

In order to check whether LjNPF8.6 plays any role in the uptake of external nitrate and/or the distribution of this nutrient to different plant tissues, we compared the nitrate content of different organs in wild-type and *Ljnpf8.6* mutant plants. The analyses were conducted at 4 wpi in plants grown in the presence of 1 mM $KNO_3$. The comparison of nitrate content either in roots or leaves of wild-type and mutant plants did not show significant differences, confirming that LjNPF8.6 plays a role strictly related to nodule functionality (Fig. 8A). In the microaerophilic condition associated with the nodule environment, the efficiency of N fixation is associated largely with nitrate-dependent respiration pathways in the NI cells (Kato et al., 2003; Meilhoc et al., 2010; Horchani et al., 2011). Therefore, we tested whether the reduced nitrogenase activity observed in the *Ljnpf8.6* mutants in low nitrate-permissive conditions (Fig. 5A) might be associated with a different nitrate content in nodules of wild-type and mutant plants. The nitrate content was quantified in detached wild-type and mutant nodules of plants inoculated on no N and 1 mM $KNO_3$ conditions and displaying the anthocyanin accumulation phenotype. The results shown in Figure 8B indicate that, independent of the presence of external nitrate supply, a significant content of this nutrient is detectable in nodule tissues and that no significant differences are observed on nitrate accumulation in nodules of wild-type and mutant plants. However, since the nitrate-dependent respiration pathway for the maintenance of the nodule energy status becomes more important in hypoxic than in normoxic conditions (Horchani et al., 2011; Hichri et al., 2015), we also tested whether the stressful phenotype displayed by the *Ljnpf8.6* null mutants at 4 wpi could qualitatively worsen in hypoxic conditions. Two-week-old wild-type and 46938 plants with the same number of nodules that do not show any anthocyanin accumulation symptoms were transferred in hydroponic cultures to reproduce the water-logged conditions that provoke hypoxic stress. Interestingly, mutant plants grown for an additional 2 weeks in hydroponic conditions show a clear-cut increase of the anthocyanin accumulation phenotype, which is clearly visible throughout the length of the stem tissue almost up to the shoot apex (80%–85% of the stem length versus 40%–45% displayed in normoxic conditions; Fig. 4, A and B), whereas wild-type plants did not show such evidently stressful symptoms (Supplemental Fig. S5).

## DISCUSSION

We report here the functional characterization of a member of the *L. japonicus* NPF family, LjNPF8.6, which plays a positive role in the symbiotic interaction through a nodule-associated function. NPF proteins represent a significant number of the NI transporters, and the qRT-PCR analysis shown in Figure 1 indicates

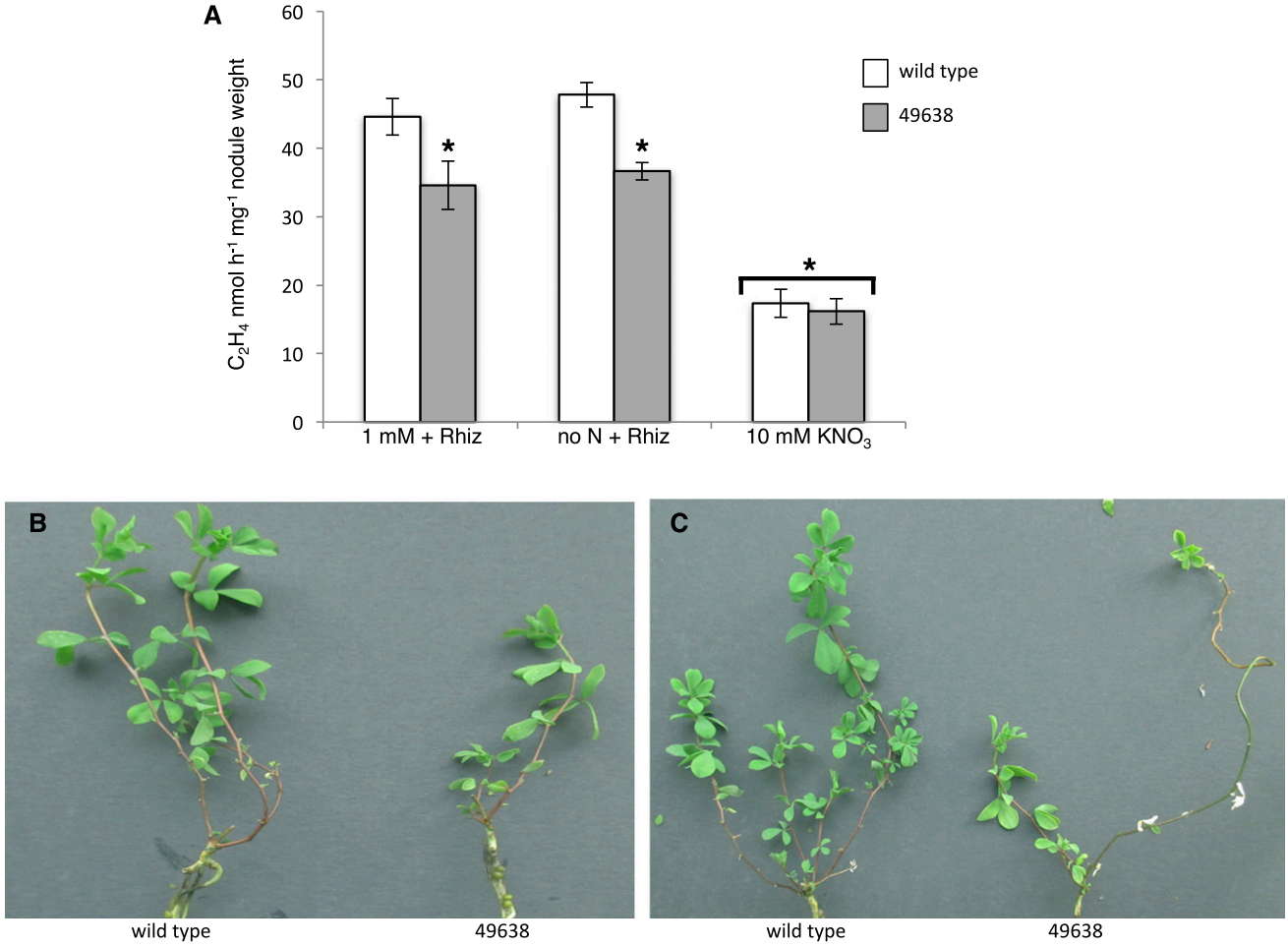


**Figure 5.** A, ARA per nodule weight of wild-type and 49638 plants. The different $KNO_3$ conditions are indicated. Data bars indicate means and SE of three independent experiments ($n = 8$ plants per experiment). Asterisks indicate significant differences ($P < 0.005$) between wild-type and 49638 nodules in no-N and 1 mM $KNO_3$ conditions. The asterisk over the bracket across the 10 mM condition indicates a significant reduction of ARA activity in nodules of both plant genotypes shifted onto high-nitrate conditions compared with nodules of plants maintained on low permissive conditions ($P < 0.001$). B and C, Representative shoot phenotypes of 8-wpi wild-type and 49638 plants transferred onto hydroponic conditions in the presence of 0.5 mM $KNO_3$ at 4 wpi. Wild-type and mutant plants were maintained in the same vessels (four vessels, 16 plants).

that LjNPF8.6 is strongly induced in nodule tissue, although it cannot be considered a strict late nodulin gene, as it is also expressed in root tissues. This result is consistent with the analysis reported by Hogslund et al. (2009), indicating that most genes functioning in mature nodule also are expressed elsewhere in the plant. The induced profile of LjNPF8.6 expression in nodules is consistent with the specific symbiotic phenotypes displayed by independent KO *Ljnpf8.6* LORE1 insertion mutants. In particular, a striking anthocyanin accumulation is observed in stems and roots of *Ljnfp8.6* mutants compared with the wild type only after *M. loti* inoculation, as no increase of pigmentation is observed in uninoculated plants grown in the presence of different nitrate concentrations (Fig. 4; Supplemental Fig. S2A). This result clearly indicates that the role played by LjNPF8.6 is strictly associated with the symbiotic program and is not related to the N nutritional status of plants linked to external nitrate availability. This is also confirmed by the analyses of nitrate content in roots and shoots that show no significant differences between wild-type and mutant plants (Fig. 8A). The production of anthocyanin is considered a hallmark of the plant response to unfavorable growth conditions (Chalker-Scott, 1999), and N limitation has been reported to trigger different anthocyanin biosynthetic pathways and accumulation in various plant tissues (Diaz et al., 2006; Rubin et al., 2009; Kovinich et al., 2014).

In the case of SNF, anthocyanin accumulation in the stem is a symptom normally exhibited by mutant plants showing an impaired N-fixation activity (Krusell et al., 2005; Ott et al., 2005; Bourcy et al., 2013). The anthocyanin accumulation phenotype is displayed in the inoculated *Ljnpf8.6* mutants by 17 to 20 d post inoculation,

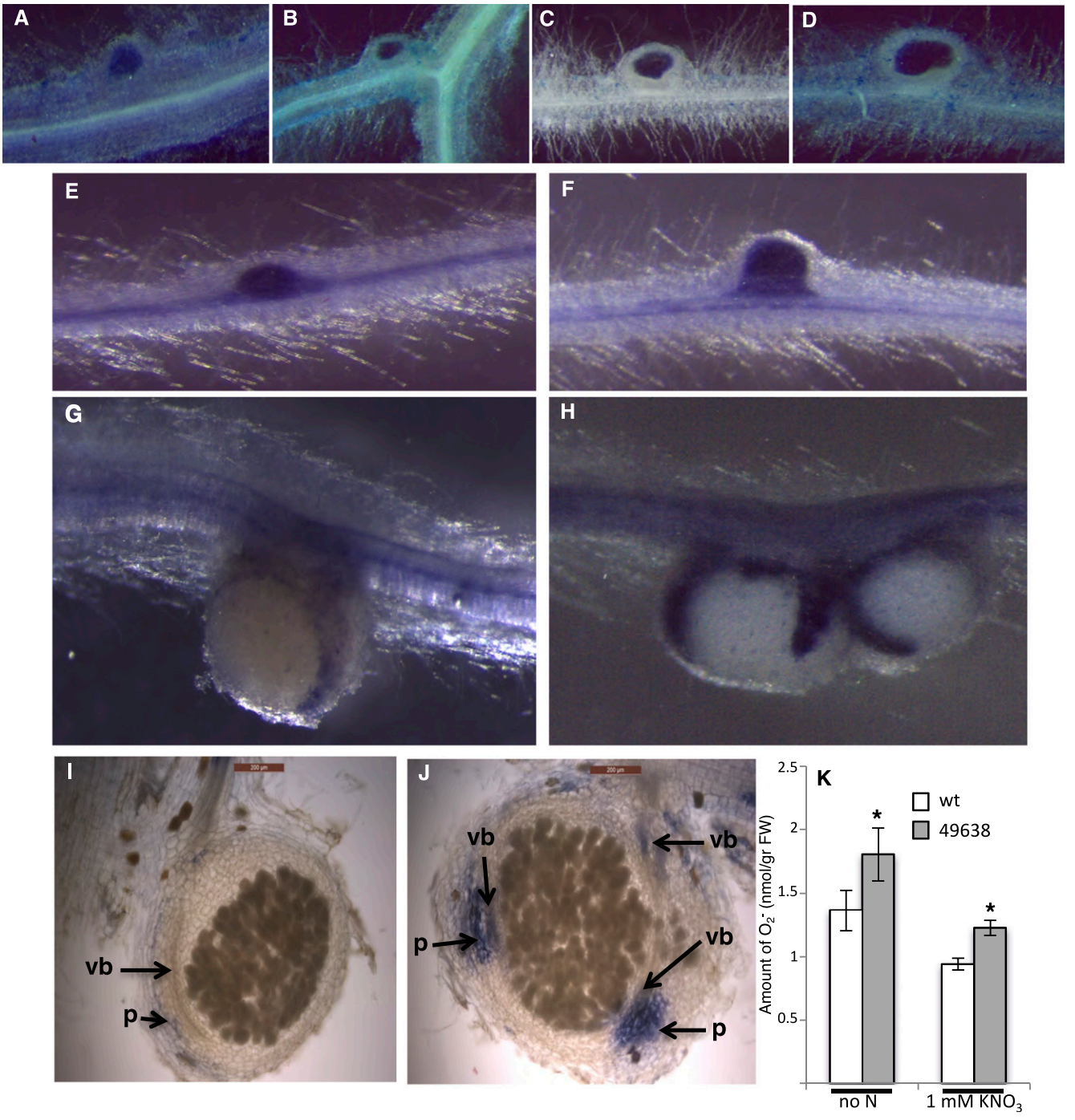


**Figure 6.** Phenotypic symbiotic characterization of *Ljnpf8.6* mutants. A to D, Histochemical detection of $\beta$-galactosidase activity to test *M. loti* (carrying the *hemA*::*lacZ*-expressing plasmid) density in young and mature nodules of wild-type (A and C) and 49638 (B and D) plants. E to H, Whole-mount NBT staining for $O_2^-$ anion detection of wild-type (E and G) and 49638 (F and H) nodule primordia and mature nodules. I and J, Sections (100 $\mu$m) of wild-type (I) and 49638 (J) mature nodules stained with NBT. Arrows indicate staining in the parenchyma (p) and nodular vascular bundles (vb). K, Quantification of NBT staining in wild-type (wt) and 49638 mutant lines. Data bars represent means and SE of nodules from three independent samples (eight plants per experiment). Asterisks indicate significant differences from wild-type values ($P < 0.05$). FW, Fresh weight.

after the observed induction of LjNPF8.6 expression in nodule tissue (Fig. 1B) and the onset of N fixation, suggesting a role in the control of nodule functioning rather than development. Interestingly, further information about the spatial profile of LjNPF8.6 in mature *L. japonicus* nodules came from a tissue-specific profiling carried out by

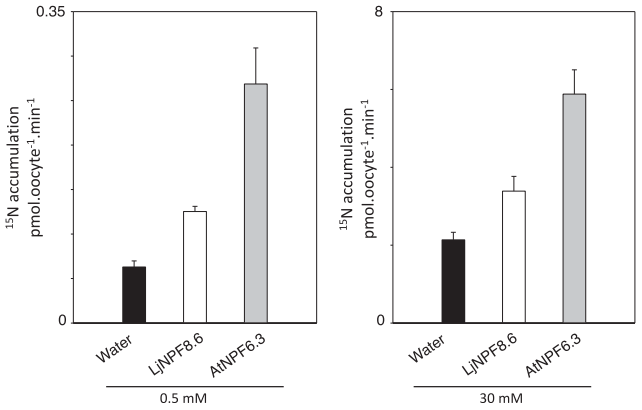


**Figure 7.** Functional expression of *LjNPF8.6* in *X. laevis* oocytes in low (0.5 mM) and high (30 mM) external nitrate concentrations. Nitrate uptake is shown in control oocytes (black bars), injected with cRNAs, expressing LjNPF8.6 (white bars) or AtNPF6.3 (gray bars; $n$ = 5–8). Values are means ± SE.

laser microdissection and microarray analysis, which revealed a specific expression of six NI NPF members, including LjNPF8.6, in the central infection zone where N fixation takes place (Takanashi et al., 2012). In particular, the LjNPF8.6 expression was not detected in the inner cortex and vascular bundle zones, suggesting for this NPF member a function associated specifically with N fixation (Takanashi et al., 2012). Consistently, *Ljnpf8.6* mutants do not show any difference, compared with wild-type plants, in the nodule formation capacity at different $KNO_3$ concentrations or in the early steps of nodule primordia invasion (Figs. 3C and 6, A–D). The direct involvement of LjNPF8.6 in the control of nodule functionality is demonstrated by the analysis reported in Figure 5A, where a significantly reduced quota of N-fixation activity (25%) is measured in mutant nodules. We also demonstrate that LjNPF8.6 does not play any role in the quick transport of external high nitrate concentration to the nodule tissues and/or sensing, which must be involved in the nitrate-dependent N-fixation inhibitory pathway (Fig. 5A; Arrese-Igor et al., 1998; Cabeza et al., 2014).

Nitrogen fixation is an extremely expensive process for legume plants, as root nodules are optional C sink organs that exploit large amounts of photosynthate resources. The partially compromised N-fixation activity displayed by the *Ljnpf8.6* mutants in the presence of low-concentration N sources (Fig. 5A) is certainly a stressful condition, which is responsible of the anthocyanin accumulation (Fig. 4; Supplemental Figs. S2A and S4), but it is still sufficient at 4 wpi to sustain a normal shoot biomass phenotype (Fig. 3, A and B). However, when plants are maintained for a longer time in symbiotic conditions, clear-cut N deficiency symptoms such as stunted shoots with pale green and/or abscised leaves are clearly displayed by the *Ljnpf8.6* mutants (Fig. 5, B and C). These phenotypes have been classified as Fix+/Fix−, associated with mutant plants with a less efficient N-fixation activity, which display N-deficiency phenotypes not as severe as in the fix− mutants (Pislariu et al., 2012).

The reduction and loss of N-fixation activity is associated with oxidative stress during the natural senescence of nodules, and similar correlated phenotypes can be observed in early senescence induced by exposure to stress conditions (Puppo et al., 2005). Therefore, the N-fixation deficiency and increased $O_2^-$ content phenotypes displayed in mature nodules of *Ljnpf8.6* mutants (Figs. 5A and 6K) are strictly associated with each other, although a cause-effect relationship can be difficult to establish. The pattern of $O_2^-$ production during nodule growth and maturation, shown in the time-course experiment displayed in Figure 6, is consistent with previous reports where NBT staining revealed $O_2^-$ accumulation in nodule primordia of indeterminate as well as determinate nodules (Fig. 6, E and F; Santos et al., 2001; Montiel et al., 2016). To our knowledge, the pattern of $O_2^-$ accumulation reported in Figure 6, G to J, has never been described in mature determinate nodules. The NBT staining indicates a predominant localization on the lenticel structures, characterized as the choke points controlling the gaseous exchanges in determinate nodules (Frazer, 1942; Pankhurst and Sprent, 1975; Jacobsen et al., 1998; Fig. 6, G and H) and the parenchyma regions (Fig. 6, I and J). Biochemical and transcriptomic analyses indicate that, in mature determinate nodules, most of the ROS-generating processes, which occur during natural or early senescence induced by exposure to stress conditions, originate in the central infected region and then spread outward (Evans et al., 1999; Puppo et al., 2005; Matamoros et al., 2013). Therefore, it is reasonable to predict the $O_2^-$ diffusion and accumulation in lenticel structures and parenchyma tissue, which are located a few cells apart from the infected zone. Furthermore, we demonstrate that the increased content of $O_2^-$ detected in the mutant plants is restricted to nodular tissue (Supplemental Fig. S2B) and, therefore, that the systemic pattern of anthocyanin accumulation (Fig. 4; Supplemental Fig. S2A) is likely not associated with a direct action of scavenging (Yamasaki et al., 1996).

Members of the NPF family may encompass different putative strategic roles associated with the control of nodule functioning, as they can transport nitrate, amino acids, peptides, dicarboxylic acids, and ABA (Frommer et al., 1994; Jeong et al., 2004; Waterworth and Bray, 2006; Kanno et al., 2012). Malate is the carbon source supplied to bacteroids for metabolism and nitrogen fixation (Day and Copeland, 1991), and in isolated soybean (*Glycine max*) symbiosomes, a carrier for monovalent dicarboxylate ions with a higher affinity for malate than for succinate has been identified (Udvardi and Day, 1997). Jeong et al. (2004) also reported the identification of an NPF gene (AgDCAT1) expressed in nodules of *A. glutinosa* encoding for a protein capable of malate transport in heterologous systems, but no further functional characterization of AgDCAT1 has been provided. The failure of LjNPF8.6 to complement the malate transport defect of

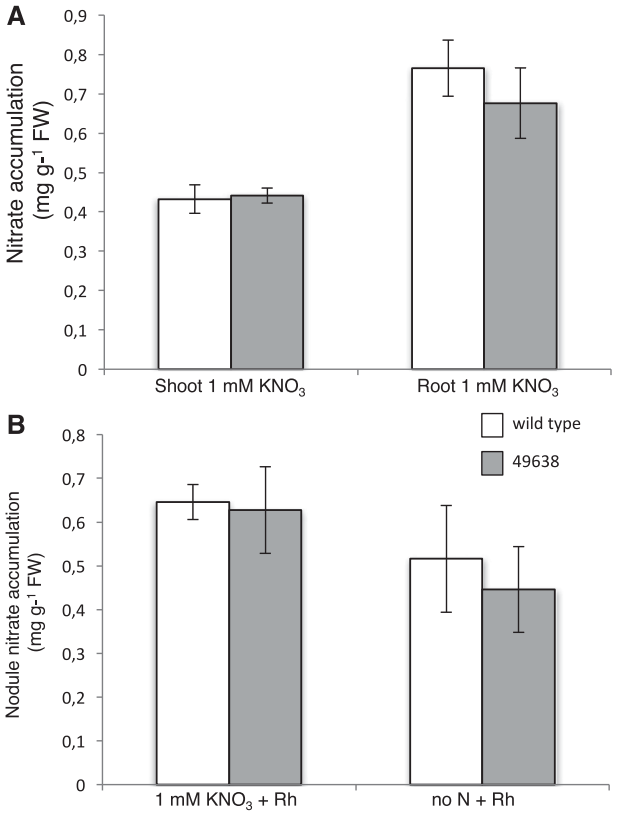


**Figure 8.** A, Nitrate content of shoots and roots from wild-type and 49638 plants grown on 1 mM $KNO_3$ and inoculated with *M. loti*. Data bars represent means and SE from three independent samples (10 plants per sample). B, Nitrate content in wild-type and 49638 4-week-old nodules. Data bars represent means and SE of nodules from three independent samples (10 plants per sample). Bars corresponding to wild-type and 49638 plants are indicated. FW, Fresh weight.

the *E. coli dctA* mutant (Supplemental Fig. S4) does not allow us to conclude that it is not involved in the C source supply to bacteroids (Day and Copeland, 1991), as we cannot exclude a nonfunctional expression of the *L. japonicus* transporter in *E. coli*. Another function that must be taken into account to explain the critical role played by LjNPF8.6 in nodule activity is related to the peptide/amino acid transport capacity. The transport of these substrates may play a positive role in supplying branched-chain amino acids necessary for bacteroid development and persistence (Prell et al., 2009) and/or for supporting polyamine biosynthesis for nitric oxide production (Gupta et al., 2011). ABA signaling also has been shown to be involved in the control of nodule functionality. However, ABA has been reported to negatively regulate N fixation in *L. japonicus*, as its reduced content obtained in low-sensitivity mutants as well as wild-type plants treated with abamine (a specific inhibitor of 9-cis-epoxycarotenoid dioxygenase) resulted in increased N-fixation activity, making unlikely the involvement of LjNPF8.6 in the nodular ABA transport/signaling pathway (Tominaga et al., 2009).

The preliminary biochemical characterization of LjNPF8.6 carried out in our work indicates that it is capable of achieving nitrate uptake in *X. laevis* oocytes at high (30 mM) and low (0.5 mM) external nitrate concentrations (Fig. 7). Importantly, the positive role played by LjNPF8.6 in nodule activity, indicated by the nitrogenase deficiency phenotype displayed by *Ljnpf8.6* mutants (Fig. 5A), is observed in plants grown in the chronic absence of N or in low permissive $KNO_3$ conditions (1 mM or less), which is consistent with the reported capacity of enhancing nitrate uptake in *X. laevis* oocytes at 0.5 mM external nitrate concentration (Fig. 7). NPF members are represented significantly in the protein fraction associated with the PBM and characterized either in *L. japonicus* or soybean nodules (Wienkoop and Saalbach., 2003; Clarke et al., 2015). In particular, the recent comprehensive sampling reported for PBM proteins in soybean has allowed the identification of five NPF members associated with PBM. Interestingly, the retrieved GmNPF8.6 protein (Glyma02g38970.1) also is a member of clade 8 and shares 69% amino acid identity with LjNPF8.6 (Clarke et al., 2015). A nitrate flux through the PBM, critical for nodule activity, was proposed previously. Anion transporters, members of the Major Facilitator Superfamily, with a selectivity preference for nitrate, have been identified in the PBM of soybean and *L. japonicus* nodules (GmN70 and LjN70), and their role in the control of ion and symbiosome membrane potential homeostasis has been postulated (Udvardi et al., 1991; Vincill et al., 2005). In addition, nitrate transport through the PBM has been proposed to be crucial for the nitrate-nitric oxide respiration process reported in nodules in microaerobic conditions, which is important for the maintenance of the energy status required for nitrogen fixation in normoxic and hypoxic conditions (Igamberdiev and Hill, 2009; Kato et al., 2010; Sánchez et al., 2010; Horchani et al., 2011). Nitrate in the cytosol and symbiosomes of invaded plant cells is produced at elevated rates (Herold and Puppo, 2005; Meilhoc et al., 2010; Horchani et al., 2011), and our analysis of nitrate content in nodule tissues confirms the presence of an active nitrate biosynthetic pathway within nodules independently of external supply (Fig. 8B), which may justify the symbiotic phenotypes detected in the *Ljnpf8.6* mutants even in the absence of external N sources (Figs. 4 and 5A). Therefore, LjNPF8.6 might play an active role in the control of nodule activity by participating in nitrate flux through the PBM (Udvardi et al., 1991; Horchani et al., 2011). In this context, the unchanged nitrate content observed in whole detached nodules of wild-type and mutant inoculated plants (Fig. 8B) is expected, as is the distribution of nitrate between different compartments of N-fixing nodule cells to be affected in the *Ljnpf8.6* background. Interestingly, we have observed an increased stressful phenotype associated with anthocyanin accumulation in *Ljnpf8.6* mutants grown under hydroponic hypoxic conditions, where achieving nitrate reduction into nitrite constitutes the main route for nitric oxide biosynthesis

(Supplemental Fig. S5; Horchani et al., 2011; Hichri et al., 2015).

## CONCLUSION

To our knowledge, LjNPF8.6 represents the first NPF protein playing a specific role in nodule functioning, as demonstrated by the description of different N-deficiency-associated phenotypes displayed by independent KO mutants in symbiotic conditions. Further experiments will be necessary to interpret its mechanism of action, taking into account different substrate specificities and the possible functional redundancy of these transporters in the nodule organ.

## MATERIALS AND METHODS

### Plant Material and Growth Conditions

All experiments were carried out with *Lotus japonicus* ecotype B-129 F14 GIFU (Handberg and Stougaard, 1992; Jiang and Gresshoff, 1997). Plants were cultivated in a growth chamber with a light intensity of 200 $\mu$mol $m^{-2}$ $s^{-1}$ at 23°C with a 16-h/8-h day/night cycle. Solid growth medium has the same composition as B5 medium (Gamborg, 1970), except that $(NH_4)_2SO_4$ and $KNO_3$ are omitted and/or substituted by different concentrations of $KNO_3$. KCl is added to the medium to replace the potassium source. The medium containing vitamins (Duchefa catalog no. G0415) is buffered with 2.5 mM MES (Duchefa catalog no. M1503.0250) and pH adjusted to 5.7 with KOH.

For hydroponic cultures, wild-type and mutant nodulated plants are transferred in the same vessels with derivative B5 liquid medium with 0.5 mM $KNO_3$ or without N sources (six plants per vessel). The medium is renewed every 4 d, when also the pH is checked and maintained within close limits (5.6–5.8) during the entire growth period.

*Mesorhizobium loti* inoculation is performed as described by Barbulova et al. (2005). For phenotypic comparisons, unsynchronized seedlings are discarded after germination. The strain R7A is used for the inoculation experiments and is grown in liquid TYR medium supplemented with rifampicin (20 mg $L^{-1}$). The *M. loti hemA*::*lacZ* strain was kindly provided by Dr. Jens Stougaard (University of Aarhus) and was grown in the same medium supplemented with rifampicin and tetracycline (20 mg $L^{-1}$).

### LORE1 Line Isolation

LORE1 lines 30053155, 30049638, and 30019899 (hereafter abbreviated as 53155, 49638, and 19899, respectively) were obtained from the LORE1 collection (Fukai et al., 2012; Urbański et al., 2012; Malolepszy et al., 2016). The plants in the segregating populations were genotyped, and the expression of homozygous plants was tested with the primers listed in Supplemental Table S1.

### Determination of ARA

Detached roots with comparable numbers of nodules are placed in glass vials. The vials are filled with an acetylene-air mixture ($C_2H_2$:air = 1:9, v/v). After 30 min of incubation at 25°C, the amount of ethylene in the gas phase is determined using a gas chromatograph (PerkinElmer Clarus 580).

For the analysis of ARA activity after a shift to high-$KNO_3$ conditions, 4-wpi nodulated plants are transferred on slanted petri dishes where roots are placed in a sandwich between two filter papers wet with Gamborg B5 liquid medium containing no $KNO_3$ or 10 mM $KNO_3$. Plants are maintained for 3 d in these conditions with filter papers wet with 20 mL of liquid medium. After 3 d, ARA activity is tested as described above.

### Estimation of Anthocyanin

Stem tissues from three plants per assay are weighed and then extracted with 99:1 methanol:HCl (v/v) at 4°C. The $OD_{530}$ and $OD_{657}$ for each sample are measured, and relative anthocyanin levels are determined with the equation $OD_{530} - (0.25 \times OD_{657}) \times$ extraction volume (mL) $\times$ 1/weight of tissue sample (g) = relative units of anthocyanin per g fresh weight of tissue.

### Determination of Nitrate Content

Colorimetric determination of nitrate content in nodule extracts followed the procedure described by Pajuelo et al. (2002). A total of 200 $\mu$L of 5% (w/v) salicylic acid in concentrated sulfuric acid is added to aliquots of 50 $\mu$L from the crude extracts and left to react for 20 min at room temperature. NaOH (4.75 mL of 2 N) is added to the reaction mixtures, and the absorbance is read at 405 nm after cooling. A calibration curve of known amounts of nitrate dissolved in the standard extraction buffer is used for analytical determinations. Controls are set up without salicylic acid.

### *LacZ* Activity and Histochemical Localization

*L. japonicus* roots isolated after *M. loti hemA*::*lacZ* infection are first gently rinsed in 50 mM $KH_2PO_4$ buffer, pH 7.2, and then fixed for 1 h with 1% paraformaldehyde (w/v) and 0.3 M mannitol in 50 mM $KH_2PO_4$ buffer, pH 7.2. The tissues are washed again with 5 mM $KH_2PO_4$ buffer, pH 7.2, and the histochemical analysis is performed according to Omrane et al. (2009). The stained nodulated roots are photographed with a Nikon microscope using bright-field and epipolarization optics.

### $O_2^-$ Staining

For $O_2^-$ staining, NBT (Sigma-Aldrich) was used. Nodulated roots are submerged in 1 mM NBT in 0.1 mM potassium phosphate buffer (pH 7.5), vacuum infiltrated for 30 s, and incubated 30 min at room temperature. NBT staining solution is removed, and stained roots are washed twice in 80% ethanol. NBT staining is repeated three times for a total of 10 nodules per experiment. For longitudinal sections, 12 nodules from independent experiments are sectioned on 100-$\mu$m-thick slices. Samples are photographed with a Nikon microscope using bright-field and epipolarization optics. For $O_2^-$ quantification, NBT-stained nodules are first ground into a fine powder and dissolved in 2 M KOH:dimethyl sulfoxide (1:1.16, v/v) followed by centrifugation at 12,000*g* for 10 m. Absorbance at 630 nm is immediately measured and then compared with a standard curve plotted from known amounts of NBT in the KOH:dimethyl sulfoxide mix (Ramel et al., 2009). Experiments are conducted on three biological replicates for a total of 40 nodules per genotype.

### Real-Time qRT-PCR

Real-time PCR was performed with the DNA Engine Opticon 2 System (MJ Research) using SYBR to monitor double-stranded DNA synthesis. The procedure is described by Rogato et al. (2008). The UBI gene (AW719589) was used as an internal standard. The concentration of primers was optimized for every PCR, and amplifications were carried out in triplicate. The PCR program used was as follows: 95°C for 3 min and 39 cycles of 94°C for 15 s, 60°C for 15 s, and 72°C for 15 s. Data were analyzed using Opticon Monitor Analysis Software version 2.01 (MJ Research). The qRT-PCR data were analyzed using the comparative Ct method. The relative level of expression is calculated with the following formula: relative expression ratio of the gene of interest is $2^{-\Delta CT}$, where $\Delta CT = CT_{GENE} - CT_{UBI}$. The efficiency of the LjNPF8.6 primers is assumed to be 2. Analysis of the melting curve of the PCR product at the end of the PCR run revealed a single narrow peak for each amplification product, and fragments amplified from total cDNA were gel purified and sequenced to ensure accuracy and specificity. The oligonucleotides used for the qRT-PCR are listed in Supplemental Table S1.

### Plasmid Preparation

The plasmid for the expression in *Xenopus laevis* oocytes was prepared in the following way. cDNA prepared from nodule RNA was amplified with a forward primer containing the *Bam*HI site in combination with a reverse primer containing the *Eco*RI site (Supplemental Table S1). The 1,713-bp fragment was double digested with *Bam*HI-*Eco*RI and subcloned into the pGEMHE plasmid containing the 5′ and 3′ untranslated regions of the *X. laevis* $\beta$-GLOBIN gene (Liman et al., 1992), predigested with *Bam*HI-*Eco*RI to obtain pGEMHE8.6. The correct coding sequence of LjNPF8.6 was verified by sequencing.

For expression in *Escherichia coli*, pGEMHE-8.6 was double digested with *Bam*HI-*Eco*RI and subcloned in pKK223-3 plasmid (Brosius and Holy, 1984) to obtain pKK-8.6. Primers for the subcloning of the Arabidopsis (*Arabidopsis thaliana*) At2G17470 gene used as a positive control in the complementation test are indicated in Supplemental Table S1.

## Functional Analysis of LjNPF8.6 in *X. laevis* Oocytes

pGEMHE-NPF8.6 was linearized with *Nhe*I and capped mRNA transcribed in vitro using the mMessage mMachine T7-ultra Kit (Life Technologies). Oocyte preparation has been described (Lacombe and Thibaud, 1998). Defolliculated oocytes are injected with 20 ng of cRNA and stored in a modified ND96 medium (2 mM KCl, 96 mM NaCl, 1 mM $MgCl_2$, 1.8 mM $CaCl_2$, 5 mM HEPES, 2.5 mM sodium pyruvate, pH 7.5, supplemented with gentamycin sulfate [50 $\mu$g $mL^{-1}$]). Two days after injection, batches of 10 injected oocytes are incubated in 1 mL of modified ND96 solution at pH 5.5 supplemented with 30 or 5 mM $^{15}NO_3$ supplied as $K^{15}NO_3$ for 2 h at 18°C. Oocytes are then rinsed five times in 15 mL of cold modified ND96 solution. Batches of two oocytes are then analyzed for total N content and atomic percent $^{15}N$ abundance by continuous-flow mass spectrometry, using a Euro-EA Eurovector elementar analyzer coupled with an IsoPrime mass spectrometer (GV Instruments). Oocytes injected with AtNPF6.3 cRNA and water were used as positive and negative controls, respectively. The results are presented as NPF-dependent nitrate accumulation (total $^{15}N$ in injected oocytes – $^{15}N$ in water-injected oocytes) normalized by the accumulation in 30 mM nitrate.

## Complementation of *E. coli*

*E. coli* K-12 (DCT) and its dicarboxylate transport mutant strain CBR315 (CGSC5269) were obtained from the *E. coli* Genetic Stock Center (Yale University). The phenotypes of the transformed strains were compared on M9 medium with malate or Glc as the sole carbon source.

## Statistical Analysis

Statistical analyses were performed using the VassarStats ANOVA program.

## Supplemental Data

The following supplemental materials are available.

**Supplemental Figure S1.** Homozygous plants for LORE1 insertions into the LjNPF8.6 gene are null mutants.

**Supplemental Figure S2.** Analyses of anthocyanin content in roots of wild-type and 49638 plants and quantification of NBT staining in roots and stems of wild-type and 49638 inoculated plants.

**Supplemental Figure S3.** Effects of external nitrate concentration on $^{15}N$ accumulation in LjNPF8.6-expressing oocytes.

**Supplemental Figure S4.** Complementation test of the *E. coli dctA* mutant.

**Supplemental Figure S5.** Anthocyanin accumulation phenotype in hydroponic conditions.

**Supplemental Table S1.** Oligonucleotide sequences.

## ACKNOWLEDGMENTS

We thank the facility of Integrated Microscopy of the Institute of Genetics and Biophysics for supporting the microscopy analysis and Stefano Rubino, Sara Salvia, and Danilo Maiello for technical assistance.

Received August 23, 2017; accepted September 15, 2017; published September 20, 2017.

## LITERATURE CITED

**Appleby CA** (1984) Leghemoglobin and *Rhizobium* respiration. Annu Rev Plant Physiol Plant Mol Biol **35:** 443–478

**Arrese-Igor C, Gordon AJ, Minchin FR, Denison RF** (1998) Nitrate entry and nitrite formation in the infected region of soybean nodules. J Exp Bot **49:** 41–48

**Bagchi R, Salehin M, Adeyemo OS, Salazar C, Shulaev V, Sherrier DJ, Dickstein R** (2012) Functional assessment of the *Medicago truncatula* NIP/LATD protein demonstrates that it is a high-affinity nitrate transporter. Plant Physiol **160:** 906–916

**Barbulova A, D'Apuzzo E, Rogato A, Chiurazzi M** (2005) Improved procedures for in vitro regeneration and for phenotypical analysis in the model legume *Lotus japonicus*. Funct Plant Biol **32:** 529–536

**Barbulova A, Rogato A, D'Apuzzo E, Omrane S, Chiurazzi M** (2007) Differential effects of combined N sources on early steps of the Nod factor-dependent transduction pathway in *Lotus japonicus*. Mol Plant Microbe Interact **20:** 994–1003

**Becana M, Matamoros MA, Udvardi M, Dalton DA** (2010) Recent insights into antioxidant defenses of legume root nodules. New Phytol **188:** 960–976

**Bergensen FJ** (1996) Delivery of $O_2$ to bacteroids. Protoplasma **191:** 9–20

**Bouguyon E, Brun F, Meynard D, Kubeš M, Pervent M, Leran S, Lacombe B, Krouk G, Guiderdoni E, Zažímalová E, et al** (2015) Multiple mechanisms of nitrate sensing by Arabidopsis nitrate transceptor NRT1.1. Nat Plants **1:** 15015

**Bourcy M, Brocard L, Pislariu CI, Cosson V, Mergaert P, Tadege M, Mysore KS, Udvardi MK, Gourion B, Ratet P** (2013) Medicago truncatula DNF2 is a PI-PLC-XD-containing protein required for bacteroid persistence and prevention of nodule early senescence and defense-like reactions. New Phytol **197:** 1250–1261

**Brosius J, Holy A** (1984) Regulation of ribosomal RNA promoters with a synthetic lac operator. Proc Natl Acad Sci USA **81:** 6929–6933

**Cabeza R, Koester B, Liese R, Lingner A, Baumgarten V, Dirks J, Salinas-Riester G, Pommerenke C, Dittert K, Schulze J** (2014) An RNA sequencing transcriptome analysis reveals novel insights into molecular aspects of the nitrate impact on the nodule activity of *Medicago truncatula*. Plant Physiol **164:** 400–411

**Carroll B, Gresshoff PM** (1983) Nitrate inhibition of nodulation and nitrogen fixation in white clover. Z Pflanzenphysiol **110:** 69–76

**Carroll B, Mathews A** (1990) Nitrate inhibition of nodulation in legumes. *In* PM Gresshoff, ed, Molecular Biology of Symbiotic Nitrogen Fixation. CRC Press, Boca Raton, FL, pp 159–180

**Chalker-Scott L** (1999) Environmental significance of anthocyanins in plant stress responses. Photochem Photobiol **70:** 1–9

**Chiba Y, Shimizu T, Miyakawa S, Kanno Y, Koshiba T, Kamiya Y, Seo M** (2015) Identification of *Arabidopsis thaliana* NRT1/PTR FAMILY (NPF) proteins capable of transporting plant hormones. J Plant Res **128:** 679–686

**Clarke VC, Loughlin PC, Gavrin A, Chen C, Brear EM, Day DA, Smith PMC** (2015) Proteomic analysis of the soybean symbiosome identifies new symbiotic proteins. Mol Cell Proteomics **14:** 1301–1322

**Colebatch G, Desbrosses G, Ott T, Krusell L, Montanari O, Kloska S, Kopka J, Udvardi MK** (2004) Global changes in transcription orchestrate metabolic differentiation during symbiotic nitrogen fixation in *Lotus japonicus*. Plant J **39:** 487–512

**Corratgé-Faillie C, Lacombe B** (2017) Substrate (un)specificity of Arabidopsis NRT1/PTR FAMILY (NPF) proteins. J Exp Bot **68:** 3107–3113

**Criscuolo G, Valkov VT, Parlati A, Alves LM, Chiurazzi M** (2012) Molecular characterization of the *Lotus japonicus* NRT1(PTR) and NRT2 families. Plant Cell Environ **35:** 1567–1581

**Day DA, Copeland L** (1991) Carbon metabolism and compartmentation in nitrogen-fixing legume nodules. Plant Physiol Biochem **29:** 185–201

**Diaz C, Saliba-Colombani V, Loudet O, Belluomo P, Moreau L, Daniel-Vedele F, Morot-Gaudry JF, Masclaux-Daubresse C** (2006) Leaf yellowing and anthocyanin accumulation are two genetically independent strategies in response to nitrogen limitation in *Arabidopsis thaliana*. Plant Cell Physiol **47:** 74–83

**Evans PJ, Gallesi D, Mathieu C, Hemàndez MJ, de Felipe M, Halliwell B, Puppo A** (1999) Oxidative stress occurs during soybean nodule senescence. Planta **208:** 73–79

**Frazer HL** (1942) The occurrence of endodermis in leguminous root nodules and its effect upon nodule function. Proc R Soc Edinb [Biol] **61:** 328–343

**Frommer WB, Hummel S, Rentsch D** (1994) Cloning of an Arabidopsis histidine transporting protein related to nitrate and peptide transporters. FEBS Lett **347:** 185–189

**Fujikake H, Yamazaki A, Ohtake N, Sueyoshi K, Matsuhashi S, Ito T, Mizuniwa C, Kume T, Hashimoto S, Ishioka NS, et al** (2003) Quick and reversible inhibition of soybean root nodule growth by nitrate involves a decrease in sucrose supply to nodules. J Exp Bot **54:** 1379–1388

**Fukai E, Soyano T, Umehara Y, Nakayama S, Hirakawa H, Tabata S, Sato S, Hayashi M** (2012) Establishment of a *Lotus japonicus* gene tagging population using the exon-targeting endogenous retrotransposon LORE1. Plant J **69:** 720–730

**Gamborg OL** (1970) The effects of amino acids and ammonium on the growth of plant cells in suspension culture. Plant Physiol **45:** 372–375

**Gupta KJ, Fernie AR, Kaiser WM, van Dongen JT** (2011) On the origins of nitric oxide. Trends Plant Sci **16:** 160–168

**Handberg K, Stougaard J** (1992) *Lotus japonicus*, an autogamous, diploid legume species for classical and molecular genetics. Plant J **2:** 487–496

**Hernandez-Jimenez MJ, Lucas MM, de Felipe RM** (2002) Antioxidant defence and damages in senescing lupin nodules. Plant Physiol Biochem **40:** 645–657

**Herold S, Puppo A** (2005) Oxyleghemoglobin scavenges nitrogen monoxide and peroxynitrite: a possible role in functioning nodules? J Biol Inorg Chem **10:** 935–945

**Hichri I, Boscari A, Castella C, Rovere M, Puppo A, Brouquisse R** (2015) Nitric oxide: a multifaceted regulator of the nitrogen-fixing symbiosis. J Exp Bot **66:** 2877–2887

**Ho CH, Lin SH, Hu HC, Tsay YF** (2009) CHL1 functions as a nitrate sensor in plants. Cell **138:** 1184–1194

**Hogslund N, Radutoiu S, Krusell L, Voroshilova V, Hannah MA, Goffard N, Sanchez DH, Lippold F, Ott T, Sata S, et al** (2009) Dissection of symbiosis and organ development by integrated transcriptome analysis of Lotus japonicus mutant and wild-type plants. PLoS ONE **4:** e6556

**Horchani F, Prévot M, Boscari A, Evangelisti E, Meilhoc E, Bruand C, Raymond P, Boncompagni E, Aschi-Smiti S, Puppo A, et al** (2011) Both plant and bacterial nitrate reductases contribute to nitric oxide production in *Medicago truncatula* nitrogen-fixing nodules. Plant Physiol **155:** 1023–1036

**Igamberdiev AU, Hill RD** (2009) Plant mitochondrial function during anaerobiosis. Ann Bot (Lond) **103:** 259–268

**Jacobsen KR, Rousseau RA, Denison RF** (1998) Tracing the path of oxygen into birdsfoot trefoil and alfalfa nodules using iodine vapor. Bot Acta **111:** 193–203

**Jeong J, Suh S, Guan C, Tsay YF, Moran N, Oh CJ, An CS, Demchenko KN, Pawlowski K, Lee Y** (2004) A nodule-specific dicarboxylate transporter from alder is a member of the peptide transporter family. Plant Physiol **134:** 969–978

**Jeudy C, Ruffel S, Freixes S, Tillard P, Santoni AL, Morel S, Journet EP, Duc G, Gojon A, Lepetit M, et al** (2010) Adaptation of *Medicago truncatula* to nitrogen limitation is modulated via local and systemic nodule developmental responses. New Phytol **185:** 817–828

**Jiang Q, Gresshoff PM** (1997) Classical and molecular genetics of the model legume *Lotus japonicus*. Mol Plant Microbe Interact **10:** 59–68

**Kanno Y, Hanada A, Chiba Y, Ichikawa T, Nakazawa M, Matsui M, Koshiba T, Kamiya Y, Seo M** (2012) Identification of an abscisic acid transporter by functional screening using the receptor complex as a sensor. Proc Natl Acad Sci USA **109:** 9653–9658

**Kato K, Kanahama K, Kanayama Y** (2010) Involvement of nitric oxide in the inhibition of nitrogenase activity by nitrate in Lotus root nodules. J Plant Physiol **167:** 238–241

**Kato K, Okamura Y, Kanahama K, Kanayama Y** (2003) Nitrate-independent expression of plant nitrate reductase in *Lotus japonicus* root nodules. J Exp Bot **54:** 1685–1690

**Kovinich N, Kayanja G, Chanoca A, Riedl K, Otegui MS, Grotewold E** (2014) Not all anthocyanins are born equal: distinct patterns induced by stress in Arabidopsis. Planta **240:** 931–940

**Krapp A, David LC, Chardin C, Girin T, Marmagne A, Leprince AS, Chaillou S, Ferrario-Méry S, Meyer C, Daniel-Vedele F** (2014) Nitrate transport and signalling in Arabidopsis. J Exp Bot **65:** 789–798

**Krouk G, Lacombe B, Bielach A, Perrine-Walker F, Malinska K, Mounier E, Hoyerova K, Tillard P, Leon S, Ljung K, et al** (2010) Nitrate-regulated auxin transport by NRT1.1 defines a mechanism for nutrient sensing in plants. Dev Cell **18:** 927–937

**Krusell L, Krause K, Ott T, Desbrosses G, Krämer U, Sato S, Nakamura Y, Tabata S, James EK, Sandal N, et al** (2005) The sulfate transporter SST1 is crucial for symbiotic nitrogen fixation in *Lotus japonicus* root nodules. Plant Cell **17:** 1625–1636

**Lacombe B, Thibaud JB** (1998) Evidence for a multi-ion pore behavior in the plant potassium channel KAT1. J Membr Biol **166:** 91–100

**Léran S, Varala K, Boyer JC, Chiurazzi M, Crawford N, Daniel-Vedele F, David L, Dickstein R, Fernandez E, Forde B, et al** (2014) A unified nomenclature of NITRATE TRANSPORTER 1/PEPTIDE TRANSPORTER family members in plants. Trends Plant Sci **19:** 5–9

**Liman ER, Tytgat J, Hess P** (1992) Subunit stoichiometry of a mammalian K $^{+}$ channel determined by construction of multimeric cDNAs. Neuron **9:** 861–871

**Lin CM, Koh S, Stacey G, Yu SM, Lin TY, Tsay YF** (2000) Cloning and functional characterization of a constitutively expressed nitrate transporter gene, OsNRT1, from rice. Plant Physiol **122:** 379–388

**Liu KH, Huang CY, Tsay YF** (1999) CHL1 is a dual-affinity nitrate transporter of *Arabidopsis* involved in multiple phases of nitrate uptake. Plant Cell **11:** 865–874

**Lo TCY, Rayman MK, Sanwal BD** (1972) Transport of succinate in Escherichia coli. I. Biochemical and genetic studies of transport in whole cells. J Biol Chem **247:** 6323–6331

**Malolepszy A, Mun T, Sandal N, Gupta V, Dubin M, Urbański DF, Shan N, Bachmann A, Fukai E, Hirakawa H, et al** (2016) The LORE1 insertion mutant resource. Plant J **88:** 306–317

**Matamoros MA, Fernández-García N, Wienkoop S, Loscos J, Saiz A, Becana M** (2013) Mitochondria are an early target of oxidative modifications in senescing legume nodules. New Phytol **197:** 873–885

**Meilhoc E, Cam Y, Skapski A, Bruand C** (2010) The response to nitric oxide of the nitrogen-fixing symbiont *Sinorhizobium meliloti*. Mol Plant Microbe Interact **23:** 748–759

**Meyer S, Scholz-Starke J, De Angeli A, Kovermann P, Burla B, Gambale F, Martinoia E** (2011) Malate transport by the vacuolar AtALMT6 channel in guard cells is subject to multiple regulation. Plant J **67:** 247–257

**Miller AJ, Cramer MD** (2005) Root nitrogen acquisition and assimilation. Plant Soil **274:** 1–36

**Minchin FR** (1997) Regulation of oxygen diffusion in legume nodules. Soil Biol Biochem **29:** 881–888

**Montiel J, Arthikala MK, Cárdenas L, Quinto C** (2016) Legume NADPH oxidases have crucial roles at different stages of nodulation. Int J Mol Sci **17:** E680

**Morère-Le Paven MC, Viau L, Hamon A, Vandecasteele C, Pellizzaro A, Bourdin C, Laffont C, Lapied B, Lepetit M, Frugier F, et al** (2011) Characterization of a dual-affinity nitrate transporter MtNRT1.3 in the model legume *Medicago truncatula*. J Exp Bot **62:** 5595–5605

**Naudin C, Corre-Hellou G, Voisin AS, Oury V, Salon C, Crozat Y, Jeuffroy MH** (2011) Inhibition and recovery of symbiotic $N_2$ fixation by peas (*Pisum sativum* L.) in response to short-term nitrate exposure. Plant Soil **346:** 275–287

**Noguero M, Lacombe B** (2016) Transporters involved in root nitrate uptake and sensing by Arabidopsis. Front Plant Sci **7:** 1391

**Nour-Eldin HH, Andersen TG, Burow M, Madsen SR, Jørgensen ME, Olsen CE, Dreyer I, Hedrich R, Geiger D, Halkier BA** (2012) NRT/PTR transporters are essential for translocation of glucosinolate defence compounds to seeds. Nature **488:** 531–534

**Omrane S, Chiurazzi M** (2009) A variety of regulatory mechanisms are involved in the nitrogen-dependent modulation of the nodule organogenesis program in legume roots. Plant Signal Behav **4:** 1066–1068

**Omrane S, Ferrarini A, D'Apuzzo E, Rogato A, Delledonne M, Chiurazzi M** (2009) Symbiotic competence in *Lotus japonicus* is affected by plant nitrogen status: transcriptomic identification of genes affected by a new signalling pathway. New Phytol **183:** 380–394

**Ott T, van Dongen JT, Günther C, Krusell L, Desbrosses G, Vigeolas H, Bock V, Czechowski T, Geigenberger P, Udvardi MK** (2005) Symbiotic leghemoglobins are crucial for nitrogen fixation in legume root nodules but not for general plant growth and development. Curr Biol **15:** 531–535

**Pajuelo P, Pajuelo E, Orea A, Romero JM, Marquez AJ** (2002) Influence of plant age and growth conditions on nitrate assimilation in roots of *Lotus japonicus* plants. Funct Plant Biol **29:** 485–494

**Pankhurst CE, Sprent JI** (1975) Surface features of soybean root nodules. Protoplasma **85:** 58–98

**Pislariu CI, Murray JD, Wen J, Cosson V, Muni RRD, Wang M, Benedito VA, Andriankaja A, Cheng X, Jerez IT, et al** (2012) A *Medicago truncatula* tobacco retrotransposon insertion mutant collection with defects in nodule development and symbiotic nitrogen fixation. Plant Physiol **159:** 1686–1699

**Prell J, White JP, Bourdes A, Bunnewell S, Bongaerts RJ, Poole PS** (2009) Legumes regulate Rhizobium bacteroid development and persistence by the supply of branched-chain amino acids. Proc Natl Acad Sci USA **106:** 12477–12482

**Puppo A, Groten K, Bastian F, Carzaniga R, Soussi M, Lucas MM, de Felipe MR, Harrison J, Vanacker H, Foyer CH** (2005) Legume nodule senescence: roles for redox and hormone signalling in the orchestration of the natural aging process. New Phytol **165:** 683–701

**Ramel F, Sulmon C, Bogard M, Couée I, Gouesbet G** (2009) Differential patterns of reactive oxygen species and antioxidative mechanisms during atrazine injury and sucrose-induced tolerance in *Arabidopsis thaliana* plantlets. BMC Plant Biol **9:** 28

**Rogato A, D'Apuzzo E, Barbulova A, Omrane S, Stedel C, Simon-Rosin U, Katinakis P, Flemetakis M, Udvardi M, Chiurazzi M** (2008) Tissue-specific down-regulation of *LjAMT1;1* compromises nodule function and enhances nodulation in *Lotus japonicus*. Plant Mol Biol **68:** 585–595

**Rubin G, Tohge T, Matsuda F, Saito K, Scheible WR** (2009) Members of the LBD family of transcription factors repress anthocyanin synthesis and affect additional nitrogen responses in *Arabidopsis*. Plant Cell **21:** 3567–3584

**Saito H, Oikawa T, Hamamoto S, Ishimaru Y, Kanamori-Sato M, Sasaki-Sekimoto Y, Utsumi T, Chen J, Kanno Y, Masuda S, et al** (2015) The jasmonate-responsive GTR1 transporter is required for gibberellin-mediated stamen development in Arabidopsis. Nat Commun **6:** 6095–7006

**Sánchez C, Gates AJ, Meakin GE, Uchiumi T, Girard L, Richardson DJ, Bedmar EJ, Delgado MJ** (2010) Production of nitric oxide and nitrosylleghemoglobin complexes in soybean nodules in response to flooding. Mol Plant Microbe Interact **23:** 702–711

**Santos R, Hérouart D, Sigaud S, Touati D, Puppo A** (2001) Oxidative burst in alfalfa-*Sinorhizobium meliloti* symbiotic interaction. Mol Plant Microbe Interact **14:** 86–89

**Sato S, Nakamura Y, Kaneko T, Asamizu E, Kato T, Nakao M, Sasamoto S, Watanabe A, Ono A, Kawashima K, et al** (2008) Genome structure of the legume, *Lotus japonicus*. DNA Res **15:** 227–239

**Schauser L, Roussis A, Stiller J, Stougaard J** (1999) A plant regulator controlling development of symbiotic root nodules. Nature **402:** 191–195

**Schuller KA, Minchin FR, Gresshoff PM** (1988) Nitrogenase activity and oxygen diffusion in nodules of soybean cv Bragg and a supernodulating mutant: effects of nitrate. J Exp Bot **39:** 865–877

**Takanashi K, Takahashi H, Sakurai N, Sugiyama A, Suzuki H, Shibata D, Nakazono M, Yazaki K** (2012) Tissue-specific transcriptome analysis in nodules of *Lotus japonicus*. Mol Plant Microbe Interact **25:** 869–876

**Tal I, Zhang Y, Jørgensen ME, Pisanty O, Barbosa ICR, Zourelidou M, Regnault T, Crocoll C, Olsen CE, Weinstain R, et al** (2016) The Arabidopsis NPF3 protein is a GA transporter. Nat Commun **7:** 11486–11497

**Teillet A, Garcia J, de Billy F, Gherardi M, Huguet T, Barker DG, de Carvalho-Niebel F, Journet EP** (2008) api, a novel *Medicago truncatula* symbiotic mutant impaired in nodule primordium invasion. Mol Plant Microbe Interact **21:** 535–546

**Tominaga A, Nagata M, Futsuki K, Abe H, Uchiumi T, Abe M, Kucho K, Hashiguchi M, Akashi R, Hirsch AM, et al** (2009) Enhanced nodulation and nitrogen fixation in the abscisic acid low-sensitive mutant *enhanced nitrogen fixation1* of *Lotus japonicus*. Plant Physiol **151:** 1965–1976

**Tsay YF, Chiu CC, Tsai CB, Ho CH, Hsu PK** (2007) Nitrate transporters and peptide transporters. FEBS Lett **581:** 2290–2300

**Udvardi MK, Day DA** (1997) Metabolite transport across symbiotic membranes of legume nodules. Annu Rev Plant Physiol Plant Mol Biol **48:** 493–523

**Udvardi MK, Lister DL, Day DA** (1991) ATPase activity and anion transport across the peribacteroid membrane of isolated soybean symbiosomes. Arch Microbiol **156:** 362–366

**Urbański DF, Małolepszy A, Stougaard J, Andersen SU** (2012) Genome-wide LORE1 retrotransposon mutagenesis and high-throughput insertion detection in *Lotus japonicus*. Plant J **69:** 731–741

**Valkov TV, Chiurazzi M** (2014) Nitrate transport and signaling. *In* S Tabata, J Stougaard, eds, The *Lotus japonicus* Genome: Compendium of Plant Genomes. Springer-Verlag, Berlin, pp 125–136

**Vessey JK, Waterer J** (1992) In search of the mechanism of nitrate inhibition of nitrogenase activity in legume nodules: recent developments. Physiol Plant **84:** 171–176

**Vincill ED, Szczyglowski K, Roberts DM** (2005) GmN70 and LjN70. Anion transporters of the symbiosome membrane of nodules with a transport preference for nitrate. Plant Physiol **137:** 1435–1444

**Walch-Liu P, Ivanov II, Filleur S, Gan Y, Remans T, Forde BG** (2006) Nitrogen regulation of root branching. Ann Bot (Lond) **97:** 875–881

**Wang R, Tischner R, Gutiérrez RA, Hoffman M, Xing X, Chen M, Coruzzi G, Crawford NM** (2004) Genomic analysis of the nitrate response using a nitrate reductase-null mutant of Arabidopsis. Plant Physiol **136:** 2512–2522

**Waterworth WM, Bray CM** (2006) Enigma variations for peptides and their transporters in higher plants. Ann Bot (Lond) **98:** 1–8

**Wienkoop S, Saalbach G** (2003) Proteome analysis: novel proteins identified at the peribacteroid membrane from *Lotus japonicus* root nodules. Plant Physiol **131:** 1080–1090

**Witty JF, Minchin FR** (1998) Hydrogen measurements provide direct evidence for a variable physical barrier to gas diffusion in legume nodules. J Exp Bot **49:** 1015–1020

**Yamasaki H, Uefuji H, Sakihama Y** (1996) Bleaching of the red anthocyanin induced by superoxide radical. Arch Biochem Biophys **332:** 183–186

**Yano K, Shibata S, Chen WL, Sato S, Kaneko T, Jurkiewicz A, Sandal N, Banba M, Imaizumi-Anraku H, Kojima T, et al** (2009) CERBERUS, a novel U-box protein containing WD-40 repeats, is required for formation of the infection thread and nodule development in the legume-*Rhizobium* symbiosis. Plant J **60:** 168–180